Monthly Notices of the ROYAL ASTRONOMICAL SOCIETY

MNRAS **530,** 1506–1511 (2024) https://doi.org/10.1093/mnras/stae888
Advance Access publication 2024 March 27

The FAST Galactic Plane Pulsar Snapshot Survey – V. PSR J1901+0658 in a double neutron star system

W. Q. Su [1,2] J. L. Han [1,2,3★] Z. L. Yang,[1,2] P. F. Wang,[1,2,3] J. P. Yuan,[3,4] C. Wang,[1,2,3] D. J. Zhou [1] T. Wang,[1] Y. Yan,[1,2] W. C. Jing [1,2] N. N. Cai,[1] L. Xie,[1] J. Xu [1,3] H. G. Wang,[5,6] R. X. Xu[7] and X. P. You[8]

[1]*National Astronomical Observatories, Chinese Academy of Sciences, Jia-20 Datun Road, ChaoYang District, Beijing 100012, China*
[2]*School of Astronomy and Space Science, University of Chinese Academy of Sciences, Beijing 100049, China*
[3]*Key Laboratory of Radio Astronomy and Technology, Chinese Academy of Sciences, Beijing 100101, China*
[4]*Xinjiang Astronomical Observatory, Chinese Academy of Sciences, 150 Science 1-street, Urumqi 830011, China*
[5]*Department of Astronomy, School of Physics and Materials Science, Guangzhou University, Guangzhou 510006, Guangdong Province, China*
[6]*National Astronomical Data Center, Great Bay Area, Guangzhou 510006, Guangdong Province, China*
[7]*Department of Astronomy, Peking University, Beijing 100871, China*
[8]*School of Physical Science and Technology, Southwest University, Chongqing 400715, China*

Accepted 2024 March 25. Received 2024 March 23; in original form 2024 February 9

ABSTRACT

Double neutron star (DNS) systems offer excellent opportunities to test gravity theories. We report the timing results of PSR J1901+0658, the first pulsar discovered in the FAST Galactic Plane Pulsar Snapshot (GPPS) Survey. Based on timing observations by FAST over 5 yr, we obtain the phase-coherent timing solution and derive the precise measurements of its position, spin parameters, orbital parameters, and dispersion measure. It has a period of 75.7 ms, a period derivative of 2.169(6) $\times 10^{-19}$ s s^{-1}, and a characteristic age of 5.5 Gyr. This pulsar is in an orbit with a period of 14.45 d and an eccentricity of 0.366. One post-Keplerian parameter, periastron advance, has been well-measured as being 0.00531(9) deg yr^{-1}, from which the total mass of this system is derived to be 2.79(7) $M_\odot$. The pulsar has the mass upper limit of 1.68 $M_\odot$, so the lower limit for the companion mass is 1.11 $M_\odot$. Because PSR J1901+0658 is a partially recycled pulsar in an eccentric binary orbit with such a large companion mass, it should be in a DNS system according to the evolution history of the binary system.

Key words: binaries: general – stars: neutron – pulsars: individual: PSR J1901+0658.

1 INTRODUCTION

Double neutron star (DNS) systems are unique laboratories to test gravity theories in the strong-field regime and study binary evolution. Most DNS systems are identified from radio pulsars, enabling precise measurements of their properties, orbital characteristics, and strong-field effects using pulsar timing. The first DNS system, PSR B1913+16, was discovered by Hulse & Taylor (1975). Its orbital decay provided crucial evidence for gravitational waves, confirming a key prediction of general relativity (Taylor & Weisberg 1989). The orbital decay in some compact DNS systems leads to the final merger of two neutron stars, some have been detectable by ground-based gravitational wave detectors, e.g. GW170817 (Abbott et al. 2017).

Until now, there have been about 3500 pulsars in the Australia Telescope National Facility (ATNF) Pulsar Catalogue[1] (Manchester et al. 2005). However, only 27 of them are in DNS systems (or candidates), and 23 DNS are in the Galactic field (including five DNS candidates: PSRs J1753−2240, J1755−2550, J1759+5036, J1906+0746, and J2150+3427) with an orbital period in the range from 0.078 to 45 d and an eccentricity in the range from 0.064 to 0.828. Radio pulsars in most DNS systems are partially recycled, with a period in the range from 16.9 to 185 ms and a period derivative in the range from 2.7×10^{-20} to 1.8×10^{-17} s s^{-1}. In general, as long as two post-Keplerian (PK) parameters are measured, the masses of two neutron stars in a DNS system as well as the orbital inclination can be determined (e.g. Lorimer & Kramer 2004). The measurements of multiple PK parameters certainly enable a precise test of gravity theories. For example Kramer et al. (2021) achieved the most precise confirmation of the general relativity in the strong-field regime to date by measuring seven PK parameters of the double pulsar system, PSRs J0737−3039A and B.

DNS systems can be formed at the end of the evolution of two massive main-sequence stars (e.g. Bhattacharya & van den Heuvel 1991). The general scenario is the following. One of the stars evolves and undergoes a supernova explosion, forming a neutron star. Then the survived binary system evolves to be a high-mass X-ray binary system (e.g. Tauris & van den Heuvel 2023) until the second star expands and fills its Roche lobe, and experiences the Roche lobe overflow. In this phase, the system becomes unstable and forms a

★ E-mail: hjl@nao.cas.cn
[1]http://www.atnf.csiro.au/research/pulsar/psrcat/

© 2024 The Author(s).
Published by Oxford University Press on behalf of Royal Astronomical Society. This is an Open Access article distributed under the terms of the Creative Commons Attribution License (https://creativecommons.org/licenses/by/4.0/), which permits unrestricted reuse, distribution, and reproduction in any medium, provided the original work is properly cited.

Downloaded from https://academic.oup.com/mnras/article/530/2/1506/7636506 by National Astronomical Observatory user on 02 April 2025

Table 1. FAST observations for PSR J1901+0658.

Projects	PI	Obs. dates	FAST Obs. mode	Obs. time	No. of Obs.	No. of channels	No. of Pol.
GPPS Survey	J. L. Han	58563–59499	SnapShot	5 min	3	2048/4096	2/4
			Tracking	10 min	2	4096	4
PT2020_0071	J. P. Yuan	59152–59279	Tracking/SwiftCalibration	8 min	4	1024	4
PT2022_0047	W. Q. Su	59876–60133	SwiftCalibration	5 or 15 min	22	2048	4
PT2023_0143	Z. L. Yang	60237–60321	SwiftCalibration	5 min	2	2048	4
PT2023_0195	W. C. Jing	60353–60386	TrackingWithAngle	15 min	2	4096	4

common envelope (CE) so that the orbital angular momentum is lost efficiently and the orbit is shrunk. Afterward, the CE is ejected (Paczynski 1976; Ivanova et al. 2013), and the binary system may survive as a neutron star with a helium star companion. When the helium star evolves and fills its Roche lobe, another phase of the Roche lobe overflow occurs and the NS is spun-up (Dewi et al. 2002; Tauris, Langer & Podsiadlowski 2015). Eventually, the second star also undergoes a supernova explosion (ultrastripped supernova; Tauris et al. 2013, 2015), producing a second neutron star if the helium star is massive enough. In this case, the binary system evolves into a DNS system, featuring an old, mildly recycled pulsar and a younger canonical pulsar. They are in an eccentric orbit. An alternative scenario for the double neutron star formation is that the DNS system evolves from two stars with nearly equal masses, avoiding the need for CE evolution with a neutron star (Brown 1995; Dewi, Podsiadlowski & Sena 2006). Measuring the properties of DNS systems, such as the pulsar's spin periods, orbital periods, eccentricities, and mass distribution, provides invaluable insights into their complicated unknown evolutionary history (e.g. Tauris et al. 2017; Vigna-Gómez et al. 2018).

The Five-hundred-meter Aperture Spherical radio Telescope (FAST; Nan 2006) is currently the most sensitive single-dish radio telescope in the world. We are carrying out the FAST Galactic Plane Pulsar Snapshot (GPPS) Survey (Han et al. 2021; Zhou et al. 2023a) in the FAST visible sky region of the Galactic latitude range of $\pm 10^{\circ}$ with the 19-beam *L*-band receiver covering the frequency range of 1.0–1.5 GHz. Up to now, the FAST GPPS Survey has discovered 637 pulsars[2], including more than 76 transient pulsars (Zhou et al. 2023a), and five fast radio bursts (Zhou et al. 2023b). We have obtained the timing solutions for 30 newly discovered pulsars (Su et al. 2023). Here, we report the phase-coherent timing solution of *the first pulsar* discovered in the FAST GPPS Survey, PSR J1901+0658, which is in a binary system with a total mass of 2.79 $M_{\odot}$, the companion of this millisecond pulsar must be another neutron star.

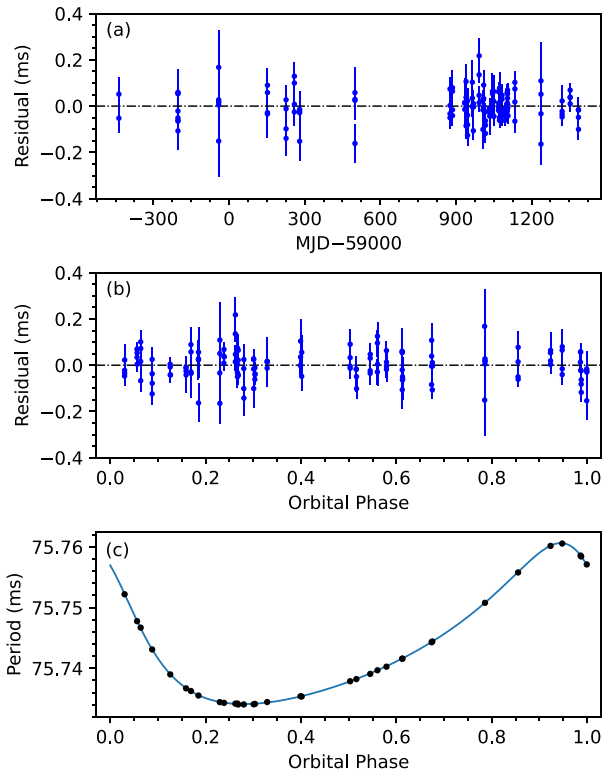


Figure 1. The post-fit timing residuals of PSR J1901+0658 for the phase-connected timing solution presented in Table 2, plotted against MJD in *sub-panel* (*a*) or the orbit phase referenced to the epoch of periastron in *sub-panel* (*b*). The apparent spin period varies with the orbit phase as shown in *sub-panel* (*c*). Error bars are included in all plots to represent uncertainties, although some are relatively small and may not be visible. The solid line is the final fitting according to the binary model.

2 FAST OBSERVATIONS AND RESULTS

PSR J1901+0658 was discovered in the first test observations on 2019 March 21 for the FAST GPPS Survey, and it was given a temporary name PSR J1901+0659g (gpps0001) in Han et al. (2021). The timing data for this pulsar have been obtained by several FAST observation projects, including PT2020_0071, PT2022_0047, PT2023_0143, and PT2023_0195, see Table 1. All observations were carried out using the FAST *L*-band 19-beam receiver in the radio frequency range of 1.0–1.5 GHz. The data are always recorded in search mode, divided into 1024, 2048, or 4096 frequency channels for the band, with a sampling time of 49.152 μs. For each frequency channel, data were collected for two polarization channels (*XX* and *YY*) during two GPPS Survey observations, G40.52+0.93_20190321 and G40.17+1.19_20200420, but for four polarization channels (*XX*, *YY*, Re[X^*Y] and Im[X^*Y]) in the remaining observations.

In the FAST GPPS Survey observations, the 'snapshot mode'[3] was designed to cover a sky area by using four nearby pointings

[2]http://zmtt.bao.ac.cn/GPPS/

[3]FAST can make observations in different modes with the 19-beam *L*-band receivers: the 'snapshot mode' covers a sky area by four pointings of the 19 beams via three beam switches, and these beams are aligned with the Galactic plane; the 'tracking mode' continuously tracks a position by the central beam (i.e. M01) for some time, with an option for possible data recording for all 19 beams which are aligned with the equator; the 'SwiftCalibration mode' leads the telescope first to point at a position 10 arcmin away from the target with the on–off calibration signals, and then tracks the target; the 'TrackingWithAngle mode' first rotates the 19-beam receiver by a given angle from the equator, and then tracks the target by the central beam, with

Downloaded from https://academic.oup.com/mnras/article/530/2/1506/7636506 by National Astronomical Observatory user on 02 April 2025

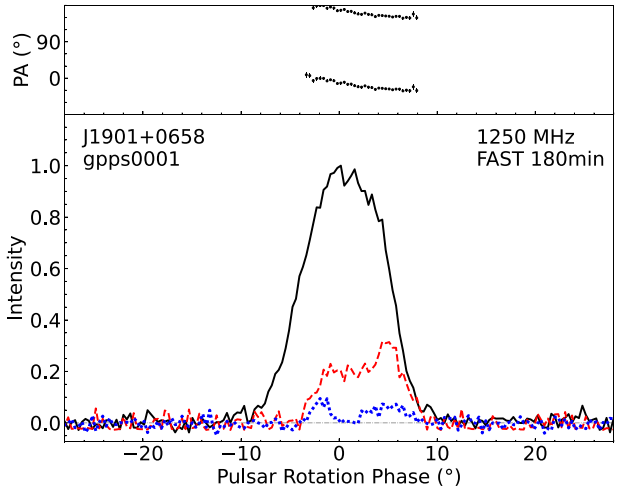


Figure 2. Polarization profile of PSR J1901+0658, showing the total intensity (solid line), linear polarization (dashed line), circular polarization (dotted line) in the *lower sub-panel*, with the polarization position angle curve displayed in the *top sub-panel*.

(Han et al. 2021), with each pointing lasting for 5 min. In the snapshot observation of G40.17+1.19_20200420, PSR J1901+0658 was detected by the beam M10 in two different pointings, P1M10 and P4M10. We also got it from the beam P3M15 in both G40.52+0.93_20190321 and G40.52+0.93_20211012. During the follow-up timing observations, PSR J1901+0658 was tracked for 5 or 15 min each session, utilizing the FAST 'Tracking mode' or 'SwiftCalibration mode'. Recently, this pulsar has been detected by the beam M11 from two 'TrackingWithAngle mode' observations, J1901+0708R-11_20240213 and J1901+0708R-11_20240317. All these data collected from the FAST GPPS Survey and follow-up observations are used together in this paper to obtain the timing solution.

With the 19-beam receiver, the FAST has a system temperature of around 22 K. In many observations, we use the periodic calibration noise signals to calibrate the system and polarization. These signals were injected for 2 min (for the 15-min tracking sessions and the snapshot observations) or 40 s (for the 5- and 8-min observation sessions) at the beginning or the end of each observation session.

All FAST observation data of PSR J1901+0658 were folded using the DSPSR[4] (van Straten & Bailes 2011), taken the initial position, period, and dispersion measure (DM) obtained from the survey. Subsequently, we used PDMP tool in the PSRCHIVE package[5] (Hotan, van Straten & Manchester 2004) to refine the optimal period and DM for each observation. The observed periods of different epochs have been Doppler-shifted, indicating the presence of a binary companion. Based on the technique presented in Bhattacharyya & Nityananda (2008), we performed a four-dimensional search to fit the measured spin periods from different epochs, as illustrated in Fig. 1(c), employing an eccentric binary orbit model. This allowed us to obtain initial values for binary parameters, including the spin period P, orbital period P_b, projected semimajor axis of orbit x, orbital eccentricity e, longitude of periastron ω_0, and epoch of periastron T_0. With these first estimated parameters, along with the position obtained during the survey and the optimal DM obtained through PDMP, we proceeded to fold the data into 10-s sub-integrations, each consisting of 1024 phase bins. We also applied PAZ and PSRZAP to diminish the radio frequency interference. Subsequently, the folded data was summed into two or four sub-integrations and two frequency channels. Utilizing the data with the highest signal-to-noise ratio (S/N), we generated a noise-free template using PAAS. Then, times of arrival (TOAs) were obtained using PAT.

We then conducted the timing analysis using the TEMPO2 package[6] (Hobbs, Edwards & Manchester 2006). The initial timing model includes the position, spin frequency ν, derivative of the spin frequency $\dot{\nu}$, P_b, x, e, ω_0, T_0, and DM, with the initial $\dot{\nu}$ set to zero.

Table 2. Measured and derived parameters for PSR J1901+0658. The 1σ uncertainty of the measured parameters is given in brackets, scaled by the square root of the reduced chi-square.

General information	
Pulsar name	J1901+0658
Data span (MJD)	58563.1–60386.0
Number of TOAs	140
Weighted rms timing residual (μs)	52.9
Reduced χ^2 value	1.5
Time units	TCB
Solar system ephemeris model	DE440
Binary model	BT
Measured parameters	
Right ascension, α (hh:mm:ss)	19:01:22.8512(3)
Declination, δ (dd:mm:ss)	+ 06:58:24.131(6)
Pulse frequency, ν (s^{-1})	13.20239193874(1)
First derivative of pulse frequency, $\dot{\nu}$ (s^{-2})	$-3.78(1) \times 10^{-17}$
Dispersion measure, DM ($cm^{-3}pc$)	125.88(1)
Epoch (MJD)	60103.7
Orbital period, P_b (d)	14.4547721(2)
Epoch of periastron, T_0 (MJD)	59265.530338(8)
Projected semi-major axis of orbit, x (lt-s)	32.40204(1)
Longitude of periastron, ω_0 (deg)	43.6259(2)
Orbital eccentricity, e	0.3662392(5)
Periastron advance, $\dot{\omega}$ (deg yr^{-1})	0.00531(9)
Derived parameters	
Spin period, P (s)	0.07574385039347(5)
Spin period derivative, $\dot{P}$ ($s\ s^{-1}$)	$2.169(6) \times 10^{-19}$
$\log_{10}$ (Characteristic age, yr)	9.74
$\log_{10}$ (Surface magnetic field strength, G)	9.61
$\log_{10}$ (Edot, ergs/s)	31.29
Mass function, f ($M_\odot$)	0.1748144(1)
Total mass, M_{tot} ($M_\odot$)	2.79(7)
DM derived distance, D_{NE2001} (kpc)	3.8
DM derived distance, D_{YMW16} (kpc)	3.8
Polarization profile parameters	
Pulse width at 50 per cent peak intensities, W_{50} (°)	9.8(4)
Pulse width at 10 per cent peak intensities, W_{10} (°)	15.1(4)
Linear polarization percentage, L/I (per cent)	23(4)
Circular polarization percentage, V/I (per cent)	4(4)
Absolute circular polarization percentage,|V|/I (per cent)	6(3)
Rotation measure, RM (rad m^{-2})	−102(1)

an option for possible data recording for all 19 beams. See the FAST web page https://fast.bao.ac.cn/cms/article/24/ for details.

[4]http://dspsr.sourceforge.net/

[5]http://psrchive.sourceforge.net

[6]http://bitbucket.org/psrsoft/tempo2

Downloaded from https://academic.oup.com/mnras/article/530/2/1506/7636506 by National Astronomical Observatory user on 02 April 2025

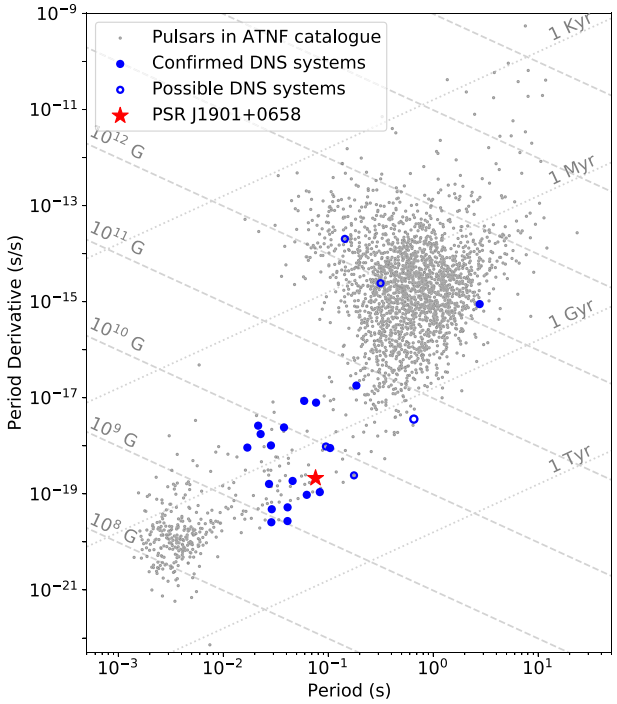


Figure 3. The $P - \dot{P}$ diagram for pulsars with indications for PSR J1901+0658 (the star) and other known DNS systems in the Galactic field (dots), DNS candidates (circles). The parameters for all known pulsars (points) are taken from the ATNF Catalogue v1.70 (Manchester et al. 2005). Data for three pulsars, PSRs J1018−1523, J1208−5936, and J2150+3427, are taken from Swiggum et al. (2023), Colom i Bernadich et al. (2023), and Wu et al. (2023). The dashed and dotted lines in the background indicate constant surface magnetic field strengths and characteristic ages, respectively.

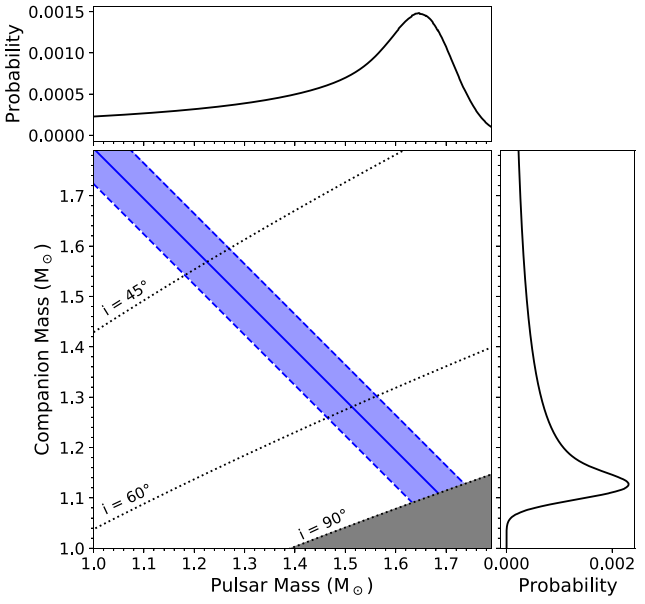


Figure 4. The mass–mass diagram for PSR J1901+0658, with probability distribution functions for the pulsar mass and companion mass in the *top* and *right sub-panels*. The probability distribution functions are calculated by assuming an isotropic orbital orientation distribution. The shaded area in the bottom right corner is an excluded parameter space defined by the mass function; the area between dashed lines is the possible parameter space constrained by the total mass derived from $\dot{\omega}$, with a uncertainty of $\pm 1\sigma$.

Our timing analysis began with these condensed data and the initially fitting ν and binary parameters. Subsequently, we fitted the new position, $\dot{\nu}$, and DM as necessary. Eventually, we introduced one of the PK parameters, the periastron advance $\dot{\omega}$, into the timing model, which was possible due to the system's significant eccentricity. Using the phase-coherent timing solution, we refolded the data and applied calibration procedures following Wang et al. (2023). The folded data was again summed into two or four sub-integrations, and all frequency channels were combined. TOAs were recalculated using the new templates derived from integrated pulse profiles, and parameters except DM were refitted to obtain the final ephemeris. The BT binary model (Blandford & Teukolsky 1976), the JPL DE440 ephemeris, and the TCB units are used in our analysis. We combined all data recorded four polarization channels with a high S/N to obtain the polarization profile for PSR J1901+0658, as shown in Fig. 2.

Based on FAST observations for 5 yr, we obtain the timing solution for PSR J1901+0658 as presented in Table 2, and the corresponding timing residuals are depicted in Figs 1(a) and (b). The timing solution includes precise measurements of the pulsar's position, spin parameters, orbital parameters, and DM. The weighted residual rms is 52.9 μs, less than 0.1 per cent of the pulsar period, indicating a good fit using the timing model. In Fig. 2, we present the polarization profiles of PSR J1901+0658 after combining all available data, folded using the timing results. The profile properties are also listed in Table 2.

3 IMPLICATIONS AND DISCUSSIONS

PSR J1901+0658 has a period of 75.7 ms and a period derivative of $2.169(6) \times 10^{-19}$ s s^{-1}. It is located in the gap between millisecond pulsars and normal pulsars in the P–$\dot{P}$ diagram as shown in Fig. 3, among typical DNS systems. According to these spin parameters, its characteristic age is estimated to be 5.5 Gyr, the surface magnetic field strength is about 4.1×10^9 G. Its period of several tens of milliseconds, the large age, and the weak magnetic field strength all indicate that it is a partially recycled pulsar, which must have experienced a short accretion process.

According to the Keplerian parameters, PSR J1901+0658 is in a binary system with significant eccentricity. It has an orbital period of 14.45 d, the eccentricity of the orbit is 0.366, and the projected semimajor axis of the orbit is 32.4 lt-s. Using these orbital parameters, we obtain the mass function of

$$f(m_{\rm p}, m_{\rm c}) = \frac{(m_{\rm c} \sin i)^3}{(m_{\rm p} + m_{\rm c})^2} = \frac{4\pi^2 x^3}{P_{\rm b}^2 T_\odot} = 0.1748144(1)\ {\rm M}_\odot, \quad (1)$$

where $T_\odot = GM_\odot c^{-3} = 4.925490947$ μs, i is the inclination angle of the orbit, and $m_{\rm p}$ and $m_{\rm c}$ are the masses of the pulsar and its companion, respectively. For pulsars in compact binary systems, the measurement of PK parameters can further constrain the masses of the pulsar and the companion. We have successfully measured one PK parameter for PSR J1901+0658, periastron advance $\dot{\omega}$, which is 0.00531(9) deg yr^{-1}. Assuming the periastron advance is caused by the general relativistic effect alone, the rate of periastron advance should be

$$\dot{\omega} = 3T_\odot^{2/3} \left(\frac{P_{\rm b}}{2\pi}\right)^{-5/3} \frac{(m_{\rm p} + m_{\rm c})^{2/3}}{1 - e^2}. \quad (2)$$

The measurement of the periastron advance tells the total mass of this system as being $M_{\rm tot} = m_{\rm p} + m_{\rm c} = 2.79(7)\ {\rm M}_\odot$.

Downloaded from https://academic.oup.com/mnras/article/530/2/1506/7636506 by National Astronomical Observatory user on 02 April 2025

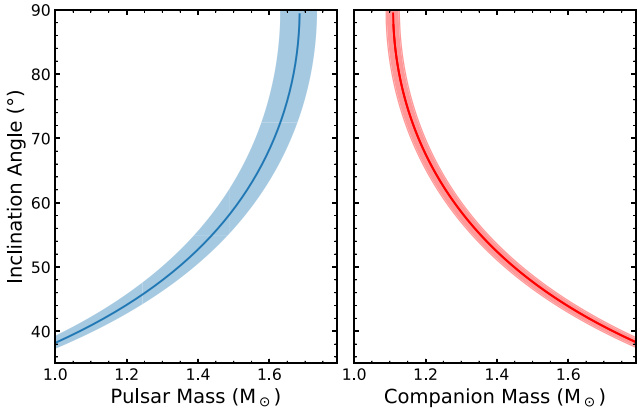


Figure 5. Possible pulsar mass (*left*) and companion mass (*right*) versus the possible orbital inclination angle, with the shaded regions for $\pm 1\sigma$.

As shown in Fig. 4, the masses of PSR J1901+0658 and its companion can be further constrained by the mass function and the total mass deduced from $\dot{\omega}$. Given that $\sin i \leq 1$, the shaded region in Fig. 4 can be ruled out. The total mass is then represented by the blue line in Fig. 4, with a shaded area for the $\pm 1\sigma$ uncertainty. Considering the upper limit of the inclination angle of $i = 90^{\circ}$, one can get the upper limit for the pulsar mass as being 1.68 $M_{\odot}$, and hence the lower limit for the companion mass as being 1.11 $M_{\odot}$. The pulsar and companion masses depend on the inclination of the orbit, as shown in Fig. 5, which cannot be constrained yet. The probability distributions for pulsar and companion masses in Fig. 4 are calculated from the $\dot{\omega}$ by assuming the isotropic orbital orientation distribution.

PSR J1901+0658 is in a wide orbit with a period of 14.4548 d, other PK parameters are hard to measure. The orbit shrink is only $\dot{P}_b = -10^{-16} \pm 10^{-10}$. For millisecond pulsars in an inclined orbit, the Shapiro delay can be measured even in wide orbits (Gautam et al. 2024). For PSR J1901+0658, the Shapiro delay can be measured only for a favourable orbital orientation and high- precision TOAs, because it would be only approximately 0.1 ms for a very edge-on orbit ($\sin i = 0.999$), while the current TOA uncertainties measured by FAST are in the range of 0.03 to 0.15 ms. The estimated value of the γ value for the Einstein term in the elliptical orbit is 0.01 s, while the available observations can limit the uncertainty to 0.17 s, far from the desired precision. Based on simulations for TOAs with such accuracy, we estimate that more than 30 yr are needed to measure the γ at a significance level exceeding 3σ.

We attempt but cannot measure the proper motion of PSR J1901+0658 from the current data available. The uncertainties or upper limit of the proper motion in right ascension and declination directions are 6 and 22 mas yr^{-1}, respectively. We cannot detect any variation of the projected semimajor axis, with an upper limit of 4×10^{-13} lt-s s^{-1}.

We searched the optical and infrared archival data, the Panoramic Survey Telescope and Rapid Response System (Pan-STARRS) Surveys (Chambers et al. 2016) and Two Micron All Sky Survey (2MASS, Skrutskie et al. 2006), for the corresponding object of the companion, but did not find a white dwarf or a main-sequence companion for this system, which further emphasizes that the companion is another neutron star.

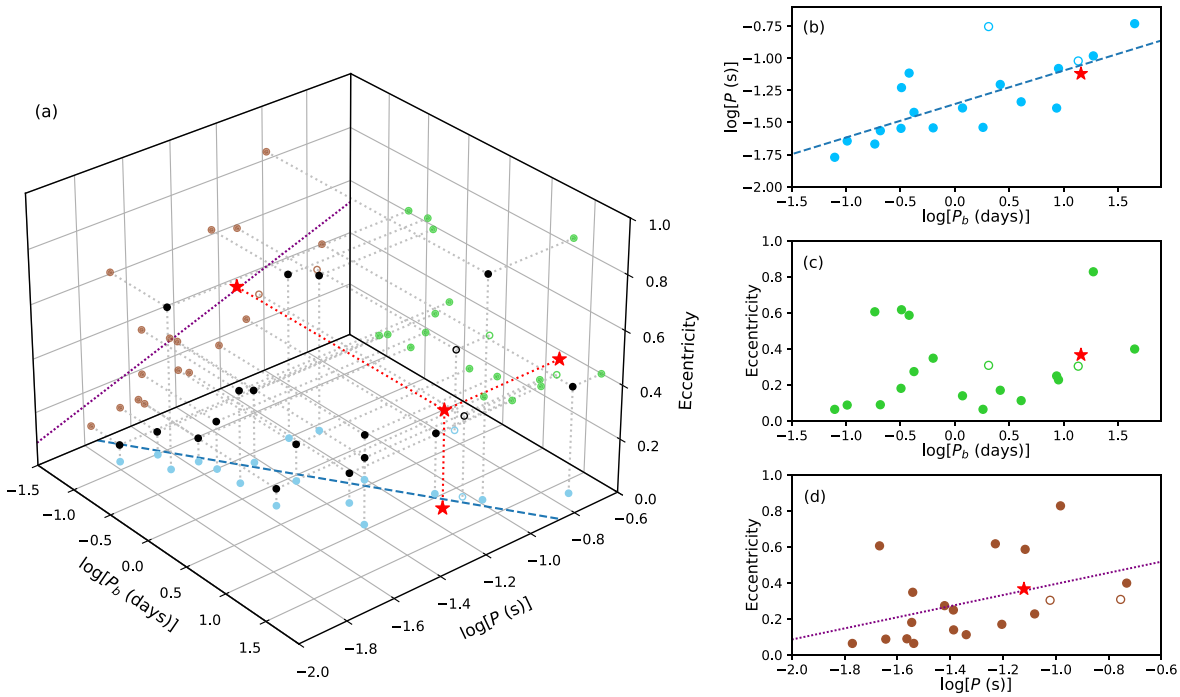


Figure 6. The distribution of orbital period, spin period, and eccentricity for recycled pulsars in DNS systems. The orbital period and spin period are well correlated, as seen in *sub-panel* (*b*), and pulsars in more elliptical orbits tend to be less recycled as seen in *sub-panel* (*d*). The correlation between orbital period and eccentricity appears very weak as seen in *sub-panel* (*c*). Previously known confirmed DNS systems (data from Manchester et al. 2005; Colom i Bernadich et al. 2023; Swiggum et al. 2023) are denoted by dots, possible DNS systems by open circle (Manchester et al. 2005), and PSR J1901+0658 by stars. The light dots represent the projections of known DNS data onto the three planes. The dashed line in the P_b−P diagram represents the relation given by Tauris et al. (2017). The dotted line is the best fit to data for spin period and eccentricity.

Downloaded from https://academic.oup.com/mnras/article/530/2/1506/7636506 by National Astronomical Observatory user on 02 April 2025

Given that this mildly recycled pulsar is in an eccentric binary orbit with a massive companion, we conclude that PSR J1901+0658 is a member of a DNS system. The second supernova explosion is needed to produce the orbit eccentricity. As mentioned in Section 1, for binaries with a wide orbit, during the previous evolution phase of a neutron star with a helium star companion, the helium star undergoes more evolution before filling its Roche lobe and initiating the mass transfer. Consequently, the neutron star has less time for accretion before the second supernova explosion, and therefore it is mildly recycled and has a relatively longer spin period. Therefore, there is a relation between the pulsar spin period P and orbit period P_b, as revealed by Tauris et al. (2017):

$$P = 44(P_{\rm b}/{\rm d})^{0.26}\ {\rm ms}. \quad (3)$$

As seen in Fig. 6(b), PSR J1901+0658 is nicely seated in the P_b–P diagram for recycled pulsars in DNS systems.

The orbit eccentricity of DNS systems also provides valuable insights into their evolutionary history. The reduced mass transfer tends to be associated with a larger envelope mass and more mass ejection during the second supernova explosion, potentially leading to a higher eccentricity. The neutron star may be kicked during the second supernova explosion that can yield a large eccentricity and a wide orbit (Tauris et al. 2015, 2017). We check the parameters, P_b, e, and P in the three-dimensional space in Fig. 6. For DNS systems in the Galactic field, as shown in Fig. 6(c), the correlation between orbital period P_b and eccentricity e is very weak.

Nevertheless, pulsars in more elliptical orbits tend to be less recycled as seen in *sub-panel* (*d*) of Fig. 6, as suggested by Faulkner et al. (2005) through the fitting of data from seven DNS systems. It is understandable in the double-star evolution scenario. During the neutron star – helium star binary stage, the less mass transfer to the neutron star results in a larger spin period, while the less mass ejection during the second supernova explosion leads to a smaller eccentricity. The electron-capture supernovae are more symmetric and produce only a smaller kick compared to core-collapse supernovae (Dewi, Podsiadlowski & Pols 2005; Tauris et al. 2015; Guo et al. 2024).

Owing to the wide orbit, PSR J1901+0658 has a merge time of more than 10^{13} yr, much longer than the Hubble time.

ACKNOWLEDGEMENTS

Observation data for this work are taken by using the FAST, a national mega-science facility of China operated by the National Astronomical Observatories, Chinese Academy of Sciences.

The FAST GPPS Survey is a key FAST science project led by JLH. He coordinated the teamwork and was finally in charge of finishing this paper. WQS processed all data presented in this paper and drafted the manuscript, under the supervision of JLH. PFW developed the processing procedures for pulsar polarization profile and pulsar timing which are extensively used in this paper. JPY, ZLY and WCJ carried out some of FAST observations presented here. CW feeds all targets for the GPPS observations. DJZ, TW, WCJ, YY, LX, and NNC contributed to different aspects of data processing and/or joined many group discussions. PFW and JX made fundamental contributions to the construction and maintenance of the computation platform. Other people jointly propose or contribute to the FAST key project. All authors contributed to the finalization of this paper.

We thank Prof. Youjun Lu for his helpful comments. The authors are supported by the National Natural Science Foundation of China (NSFC, Grant Nos 11988101 and 11833009) and the Key Research Program of the Chinese Academy of Sciences (Grant No. QYZDJ-SSW-SLH021).

DATA AVAILABILITY

Original FAST observational data will be open resources according to the FAST data 1-yr protection policy. The folded and calibrated profiles in this paper can be found on the webpage: http://zmtt.bao.ac.cn/psr-fast/.

REFERENCES

Abbott B. P. et al., 2017, Phys. Rev. Lett., 119, 161101
Bhattacharya D., van den Heuvel E. P. J., 1991, Phys. Rep., 203, 1
Bhattacharyya B., Nityananda R., 2008, MNRAS, 387, 273
Blandford R., Teukolsky S. A., 1976, ApJ, 205, 580
Brown G. E., 1995, ApJ, 440, 270
Chambers K. C. et al., 2016, preprint (arXiv:1612.05560)
Colom i Bernadich M. et al., 2023, A&A, 678, A187
Dewi J. D. M., Pols O. R., Savonije G. J., van den Heuvel E. P. J., 2002, MNRAS, 331, 1027
Dewi J. D. M., Podsiadlowski P., Pols O. R., 2005, MNRAS, 363, L71
Dewi J. D. M., Podsiadlowski P., Sena A., 2006, MNRAS, 368, 1742
Faulkner A. J. et al., 2005, ApJ, 618, L119
Gautam T., Freire P. C. C., Wu J., Venkatraman Krishnan V., Kramer M., Barr E. D., Bailes M., Cameron A. D., 2024, A&A, 682, A103
Guo Y.-L., Wang B., Chen W.-C., Li X.-D., Ge H.-W., Jiang L., Han Z.-W., 2024, MNRAS, preprint (arXiv:2401.05103)
Han J. L. et al., 2021, Res. Astron. Astrophys., 21, 107
Hobbs G. B., Edwards R. T., Manchester R. N., 2006, MNRAS, 369, 655
Hotan A. W., van Straten W., Manchester R. N., 2004, PASA, 21, 302
Hulse R. A., Taylor J. H., 1975, ApJ, 195, L51
Ivanova N. et al., 2013, A&A Rev., 21, 59
Kramer M. et al., 2021, Physical Review X, 11, 041050
Lorimer D. R., Kramer M., 2004, Handbook of Pulsar Astronomy, Vol. 4, Cambridge Univ. Press, Cambridge
Manchester R. N., Hobbs G. B., Teoh A., Hobbs M., 2005, AJ, 129, 1993
Nan R., 2006, Science in China: Physics, Mechanics and Astronomy, 49, 129
Paczynski B., 1976, in Eggleton P., Mitton S., Whelan J.eds, Proc. IAU Symp. 73, Structure and Evolution of Close Binary Systems. D. Reidel Publishing Co., Dordrecht, p. 75
Skrutskie M. F. et al., 2006, AJ, 131, 1163
Su W. Q. et al., 2023, MNRAS, 526, 2645
Swiggum J. K. et al., 2023, ApJ, 944, 154
Tauris T. M., van den Heuvel E. P. J., 2023, Physics of Binary Star Evolution. From Stars to X-ray Binaries and Gravitational Wave Sources. Princeton Univ. Press, Princeton, NJ
Tauris T. M., Langer N., Moriya T. J., Podsiadlowski P., Yoon S. C., Blinnikov S. I., 2013, ApJ, 778, L23
Tauris T. M., Langer N., Podsiadlowski P., 2015, MNRAS, 451, 2123
Tauris T. M. et al., 2017, ApJ, 846, 170
Taylor J. H., Weisberg J. M., 1989, ApJ, 345, 434
van Straten W., Bailes M., 2011, PASA, 28, 1
Vigna-Gómez A. et al., 2018, MNRAS, 481, 4009
Wang P. F. et al., 2023, Res. Astron. Astrophys., 23, 104002
Wu Q. D. et al., 2023, ApJ, 958, L17
Zhou D. J. et al., 2023a, Res. Astron. Astrophys., 23, 104001
Zhou D. J. et al., 2023b, MNRAS, 526, 2657

This paper has been typeset from a TEX/LATEX file prepared by the author.

© 2024 The Author(s).
Published by Oxford University Press on behalf of Royal Astronomical Society. This is an Open Access article distributed under the terms of the Creative Commons Attribution License (https://creativecommons.org/licenses/by/4.0/), which permits unrestricted reuse, distribution, and reproduction in any medium, provided the original work is properly cited.

Downloaded from https://academic.oup.com/mnras/article/530/2/1506/7636506 by National Astronomical Observatory user on 02 April 2025